Zuhur, Sadık; Ceylan, İlhan

Article

Energy, exergy and enviroeconomic (3E) analysis of concentrated PV and thermal system in the winter application

Energy Reports

Provided in Cooperation with:
Elsevier

Suggested Citation: Zuhur, Sadık; Ceylan, İlhan (2019) : Energy, exergy and enviroeconomic (3E) analysis of concentrated PV and thermal system in the winter application, Energy Reports, ISSN 2352-4847, Elsevier, Amsterdam, Vol. 5, pp. 262-270, https://doi.org/10.1016/j.egyr.2019.02.003

This Version is available at:
https://hdl.handle.net/10419/243581

Energy Reports 5 (2019) 262–270

Contents lists available at ScienceDirect

Energy Reports

journal homepage: www.elsevier.com/locate/egyr

Research paper

Energy, Exergy and Enviroeconomic (3E) analysis of concentrated PV and thermal system in the winter application

Sadık Zuhur [a,*], İlhan Ceylan [b]

[a] Karabuk University, Institute of Natural and Applied Sciences, 78100 Karabuk, Turkey
[b] Karabuk University, Technology Faculty, Department of Energy Systems Engineering, 78100 Karabuk, Turkey

ARTICLE INFO

Article history:
Received 27 September 2018
Received in revised form 17 November 2018
Accepted 11 February 2019
Available online xxxx

Keywords:
Concentrated PV
Solar energy
Air collector

ABSTRACT

In this study, a Concentrated Photovoltaic/Thermal (CPV/T) air collector has been designed and a prototype is produced. The purpose of this system is to meet the needs of heating and electricity of the building of application in cold winter days. The prototype which has been produced is tested with and without the use of a concentrator. The data which are obtained are exploited to carry out energy, exergy, and environmental cost analyses. During the experiments, while the average outdoor temperature was measured 10° C, the average chamber temperature was measured as 25° C for a system without a concentrator. As for the systems with a concentrator an average chamber temperature of 35° C has been obtained at approximately the same outdoor temperatures. Increasing panel backing temperature has provided a rise in chamber temperatures in winter. With the use of a concentrator, the panel back side temperatures rise and hence the efficiency of electric power production drops with respect to a system that does not employ a concentrator. However, use of a concentrator increases the thermal and electrical energy gains obtained from the system. Overall thermal energy efficiencies for the concentrated and non-concentrated systems approximately equal to 50%. Efficiencies of thermal energy of systems did not exhibit any variations. However, overall thermal energy gain has been calculated as 220 W for a system that employs a concentrator and 136 W for a system that does not.

1. Introduction

Current commercially produced photovoltaic cells convert solar energy into electrical energy with an efficiency that is lower than 20%. More than 80% of solar energy is dispersed to surroundings after conversion into electrical energy (Huang et al., 2001). Studies have been focused on hybrid photovoltaic/thermal collector (PV/T) systems in order to obtain thermal and electrical energy at low temperatures by coupling thermal collectors with photovoltaic cells in order to increase overall efficiency. On the other hand, in recent years, number of studies on solar concentrators have increased. Solar concentrators allow to focus more sunlight on the PV cells. These systems reduce the number of expensive PV cells and make the use of the sun more economical (Marques et al., 2018). Studies on these systems are reviewed below.

Joshi and Tiwari (2007) arrived at the conclusion that exergy efficiency is between 12 to 15% by using climate data for Srinagar India for 1998–2001 and creating PV/T parallel plate air collector performance for four seasons in their study (Joshi and Tiwari, 2007).

Bhowmik and Amin (2017) developed a new technology to improve the performance of the solar thermal collectors. In the study, solar reflector was used to concentrate both direct and diffuse radiation of the sun toward the collector. A prototype of a solar water heating system was constructed and obtained the improvement of the collector efficiency around 10% by using the reflector (Bhowmik and Amin, 2017).

Combined Heat and Power System (CHAPS) is a PV/Thermal system developed by Australian National University (ANU). This system is assembled by combining photovoltaic cells to produce electric power and a thermal energy absorption system to produce hot water on a concentrating parabolic trough system. The first CHAPS prototype developed for home applications had a concentration ratio of 25 while the second CHAPS system prototype had a concentration ratio of 35. They were designed to be mounted at the roofs of commercial buildings with a uniaxial monitoring system in order to contribute to the heating, cooling, and power needs. In both applications the concentrated light is focused on ribbon shaped monocrystal silicon solar cells with approximately 20% efficiency. Heat is transported via a liquid that flows through the collector where the cells are situated. Subsequently, the fluid transfers the heat to hot water storage

* Corresponding author.
E-mail address: szuhur@hotmail.com (S. Zuhur).

https://doi.org/10.1016/j.egyr.2019.02.003

Nomenclature

PV	Photovoltaic
PV/T	Photovoltaic–thermal
CPV/T	Concentrated Photovoltaic–thermal
A	Area (m^2)
c_p	Specific heat (kJ/(kg K))
$\dot{E}_l$	Rate of electrical energy (W)
$\dot{E}x_{in}$	Input exergy (W)
$\dot{E}x_{out}$	Output exergy (W)
h_{ca}	Heat transfer coefficient
I_m	Current corresponding to maximum power point (A)
$I_{(t)}$	Incident total radiation (W/m^2)
L_1	Width of the photovoltaic panel (m)
L_2	Width of the concentrator (m)
$\dot{m}$	Mass flow rate (kg/s)
$\dot{Q}$	Heat loss from the PV cell surface to the periphery (W)
$\dot{Q}_u$	Rate of useful energy transfer (W)
T	Temperature (°C)
v	Air velocity (m/s)
V_m	Voltage corresponding to maximum power point (V)
P_{CO_2}	The carbon price per kg CO_2
Z_{CO_2}	The enviroeconomic cost (CO_2 mitigation price per hour) (¢/h)

Subscript

amb	Ambient
c	Cell
i	Inflow
k	Section of the collector output channel
m	Module
o	Outlet

Greek symbols

α	Absorptivity
β	Electrical efficiency thermal coefficient
η	Efficiency
τ	Transparency
δ	Packing factor
θ	The angle between the PV module plane and the mirror plane
υ_M	The maximum incidence angle
ρ	Density (kg/m^3)
ϕ_{CO_2}	CO_2 mitigation per annum (kg CO_2 /h)
ψ_{CO_2}	The average CO_2 emission for power production by coal (kg CO_2 /kW h)

tanks by passing through a heat exchanger (Conventry et al., 2002).

Xu et al. developed a system that generates electric power and heat in a study that they carried out in 2011 in which a low concentrating photovoltaic/thermal system is used in combination with a heat pump. This system consists of a photovoltaic/thermal collector which will also be used as the evaporator of the heat pump, in which a parabolic concentrator that reflects solar light on the PV cell surface has been mounted. Refrigerant R134a flows within the multiple input flat rolled aluminum tubes which are situated under the PV cells, absorbs solar heat, and gets evaporated. Heat transferred by the refrigerant is used to heat up water in the condenser. Experiments on LCPV/T-HP (low concentrating photovoltaic/thermal-heat pump) system are conducted in Nanjing, China. Operational properties of the system are assessed by using a LCPV system with no refrigeration. Experimental results revealed that on a sunny day the COP (coefficient of performance) value is 4.8 for water to heat up from 30 °C to 70 °C with an electrical efficiency of 17.5% which is 1.36 times higher than the LCPV system. Experimental results have also demonstrated that fixed parabolic concentrators must have a concentrating ratio of 1.6 (Xu et al., 2011).

Aldegheri et al., in a study they carried out in 2014, have provided a low concentrating building-integrated solar energy system designed to produce electric power and hot water by using a Solar F-Light concentrator which was presented in International Solar Decathlon Europe (SDE) Contest for the first time in 2012. Astonyshine is a minimum energy consuming, passive, self-sustaining Mediterranean house that can produce 1380 W nominal power with a 46 photovoltaic F-Light module. In addition to this, with 6 thermal Solar F-Light module it produces 880 W of thermal power (Aldegheri et al., 2014).

Kong et al. examined the electrical and thermal outputs of a low concentrating hybrid Photovoltaic–thermal (PV/T) system that they had designed, under various weather conditions in a study they carried out in 2013. The concentrator in the system is designed by using Fresnel lenses and plane mirrors which properly concentrate sun light on solar cells. The results have shown that in a sunny day electric power production efficiency is approximately 10% and thermal efficiency is approximately 56%. Weather conditions and light intensity are important factors affecting the efficiencies. When the irradiances is above 350 W/m^2, an electrical output can be obtained and when irradiances is above 162 W/m^2, a thermal output can be obtained in the system (Kong et al., 2013).

Sharma et al. have examined phase change materials experimentally in order to increase the performances of low concentrating BICPVs (Building Integrated Concentrated Photovoltaic) through thermal arrangements in a study they carried out in 2016. The effect of PCMs (phase change materials) on electrical parameters of a BICPV system have been investigated in this study. RT42 based paraffin wax has been employed in this system. Results of experiments, which employ a 1000 W/m^2 light source indoors, indicate that inclusion of PCM increases electrical efficiency by 7.7% with respect to previous studies. When a BICPV-PCM system is compared against a system that does not employ a PCM, an average temperature drop of 3.8 °C is observed at the module center. Studies further indicate that PCM effect varies with light intensity so much so that the increases in the efficiencies of electric power production are observed to be 1.15%, 4.20%, and 6.80% at irradiances of 500, 750, and 1200 W/m^2, respectively (Sharma et al., 2016).

In this study, a concentrating photovoltaic/thermal (CPV/T) air collector is designed and fabricated to contribute to green building studies. The system aims to produce heat and electricity by utilizing the sun at the highest level using concentrator and collector. Concentrators with a theoretical ratio of concentration at 3 are used in this study. Part of the concentrated light is converted into electrical energy at the photovoltaic panel while another part is converted into thermal energy at the panel. Air heated at the collector is transported via fans supported by the panels to the space which is targeted for heating. There are many designs of PV/T air collectors in the literature. Measurements have been taken in the presence and absence of a concentrator in cold winter days in our study and the effect of using a concentrator on the system has been inspected. The system that is produced upon

a design is tried for space heating in the winter applications and as for the summer applications it will be tried for the purposes of cooling via an application of an absorption cooling/conditioning system.

2. Design and working principle

CPV/T air collector is designed as in Fig. 1. The winter application depicted in Fig. 1 is developed to meet the needs of heating and electricity of the building that it is applied in cold winter days where the sun light is scarce and is received at oblique angles and experiments on this prototype are carried out in this study. The summer application which is also depicted in Fig. 1 is our next study in line and developed to meet the needs of cooling and electricity of the building that it is applied in hot summer days. An absorbing cooling system (Cooler, Fig. 1) will be used in this system to provide cooling. The prototype which will be produced and tried in the summer months is depicted in Figs. 1 and 2. Winter application of this prototype is produced and tried in this application. Experimental set up and all of the measurements done on the system are shown in Fig. 1.

Experimental set up consists of a concentrator, an air collector, a photovoltaic panel, 2 fans, a charge regulator, an accumulator, and space targeted for heating. Produced system is shown in Fig. 3. Air collector is produced out of aluminum plates and mounted behind the photovoltaic panel. The measurements of air collector are 19 cm × 61 cm × 65 cm. The air collector system that is produced is connected to the targeted space for heating via pipes and the fans placed at the entrance/exit of the collector transported the air that is heated at the panels to the space. Air collector and pipes are insulated by glass wool and styrofoam.

Fig. 4 and Eq. (1) are exploited in the determination of size and angles of the concentrator (Hermenean et al., 2009).

$$\varepsilon = \frac{L_2}{L_1} = \frac{-\cos(2\theta + \upsilon_M)}{\cos(\theta + \upsilon_M)} \tag{1}$$

Here L_1, L_2, θ, and υ_M are the PV panel width, concentrator width, angle between the PV panel plane and the concentrator, and maximum angle of incidence of solar light, respectively. In accordance with this formula, for our design, when υ_M is 0°, $L_1 =$ 65 cm, $L_2 = 44$ cm, and $\theta = 56°$.

2.1. Working principle

In winter application which is the subject of this paper, an air collector is provided to heat the chamber. On the other hand, in the summer application, an absorbing cooling system was used to cool the chamber. In both systems, electricity is provided through concentrated PV panels. The working principles of the systems are given below.

2.1.1. Winter application

Solar light received from the concentrator impinges on photovoltaic panel and is converted into electrical energy as shown in Fig. 1. Part of this energy is spent at the fans and the rest is stored at a gel battery. When needed, this energy may be used for other purposes. Part of the concentrated light reaches the aluminum collector by penetrating its way through back of the panel. It gets heated at the panel as well. The heat so created warms the air at the collector. The air that is heated up at the collector is transported to the space targeted for heating via fans.

2.1.2. Summer application

Electrical energy obtained at the concentrators are stored at the batteries (Fig. 1, Point 8). The electrical energy that is stored operates the DC electric heater which belongs to absorption system in the ventilation channel (cooler in Fig. 1) and carries out the cooling. Cooled air in the ventilation channel is transported to the space through fans 5 and 6 as given in Fig. 1.

3. Experimental analysis

The experiments were carried out in the Tosya District of Kastamonu. The district, which is located in the northern part of Turkey, has a temperate climate in the region. The temperatures are highest on average in July, at around 20.7 °C. At −0.2 °C on average, January is the coldest month of the year. In November when the tests were carried out, the minimum temperature, the maximum temperature and the average temperature was measured as 2.6 °C, 10.2 °C and 6.4 °C (CLİMATE-DATA.ORG, 0000). There are many regions in the world and Turkey with these climatic conditions. From this point of view, similar results will be obtained in experiments with these systems in these regions. Fig. 5 shows the location of experiment was conducted and cities in Turkey with climate conditions close to the experimental conditions that did not fall below 6 °C of air temperature throughout the year.

Winter application set up which is designed and generated as depicted in Figs. 1 and 2 is examined in this research article. Experiments are performed in 2 distinct days, 1 days with a concentrator and 1 day without one. Measurements of solar radiation above and below of the concentrator, temperature at the entrance and exit of the collector and behind the panel and heated space, air speed at the collector exit, and electrical energy stored at the battery have been carried out in the experimental set up. Measurement points on the system and properties of measurement devices are given in Fig. 1 and Table 1, respectively.

4. Energy analysis

The thermal energy gain in the system, which depends on the inflow and outlet temperature of the air that is being circulated in the collector, is determined as follows.

$$\dot{Q}_u = \dot{m} c_p (T_o - T_i) \tag{2}$$

In this equation $\dot{m}$, c_p, T_i, and T_o are mass flow rate of the air that is being circulated in the system (kg/s), specific heat of the circulating air (1.007 kJ/kg K), inflow and outlet temperatures (°C) of the circulating fluid, respectively. Mass flow rate of the air that is being circulated in the system is determined as follows (Halıcı and Gündüz, 2013).

$$\dot{m} = \rho \upsilon A_k \tag{3}$$

In this equation ρ, υ, A_k are circulating air density (1.1614 kg/m^3), air velocity (m/s), and the cross section of collector exit channel (0.008 m^2) (Halıcı and Gündüz, 2013).

Electric efficiency of photovoltaics falls into two groups: module efficiency and cell efficiency. Electric losses occurred on the panels can be noticed via a change in temperature. Open circuit voltage and charging factor drops significantly with rising temperature. Besides that, short circuit current rises for a while Ceylan et al. (2016). As a result of this significant effect, cell efficiency is calculated as follows:

$$\eta_c = \eta_0 [1 - \beta(T_c - 25)] \tag{4}$$

η_0 is the efficiency under standard test conditions (STC). ($I_{(t)} =$ 1000 W/m^2, $T_c = 25$ °C AM = 1.5). T_c is the cell temperature and β is the thermal coefficient of electric efficiency. β varies depending on the material in which the solar cell is produced. It equals roughly 0.0045/K for crystal silicon, 0.0035/K for CIS, 0.0025/K for CdTe, and 0.002/K for amorphous silicon (Ceylan et al., 2016).

PV module efficiency can be calculated through the following equation.

$$\eta_m = \eta_c \cdot \tau_c \cdot \alpha_c \cdot \delta_c \tag{5}$$

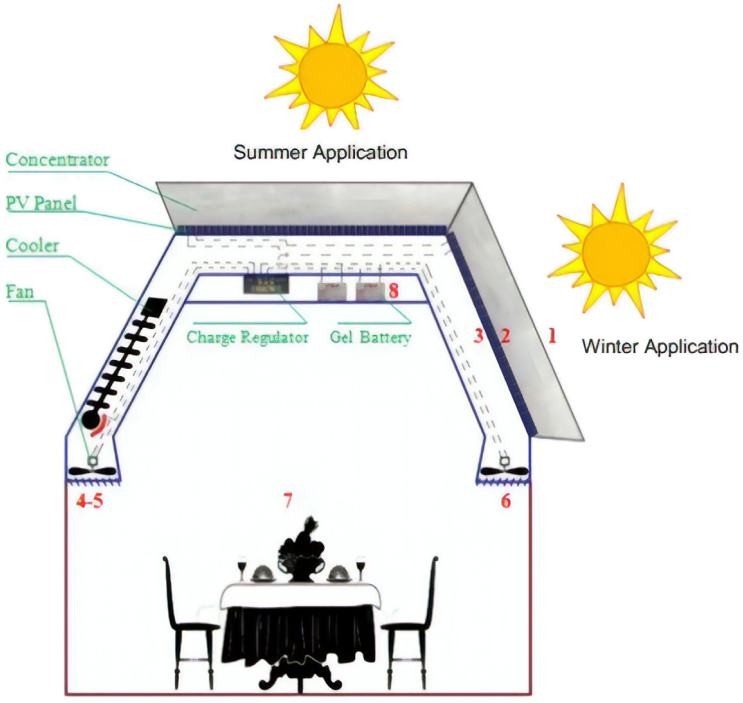

Point of measurement in the system
1: Solar Radiation
2: Solar Radiation
3: PV Panel Backing Temperature
4: Air Velocity of Collector Output
5: Air Temperature of Collector Output
6: Air Temperature of Collector Inlet
7: Chamber Temperature
8: Stored Electrical Energy in the Battery

Fig. 1. Winter and summer applications of a concentrated photovoltaic and thermal collector.

Fig. 2. (a) Summer and (b) winter applications of the system that is designed.

Table 1
Measurement devices and their properties and uncertainties.

Measurement point	Measured quantity	Device	Device properties	Uncertainty
1, 2	Solar radiation	PCE-SMP1 Data Logging Solar Power Meter - Solarmeter	0–2000 W/m^2, ±10 W/m^2	±6.0 W/m^2
3, 5, 6, 7	Temperature	MY-62 Handheld DMM Digital Multimeter-Termocouple	−20∼1000 °C, ±2.0% °C	±1.2 °C
4	Air speed	Delta Ohm HD 2303.0 - Anemometer	0.1–40 m/s, ±0.01 m/s	±0.17 m/s
8	Electric power	150 A High Precision Watt and Power Meter	0∼6554 W, ±0.1 W	±1.5 W

Fig. 3. Winter application of the concentrated photovoltaic panel/collector system, photo.

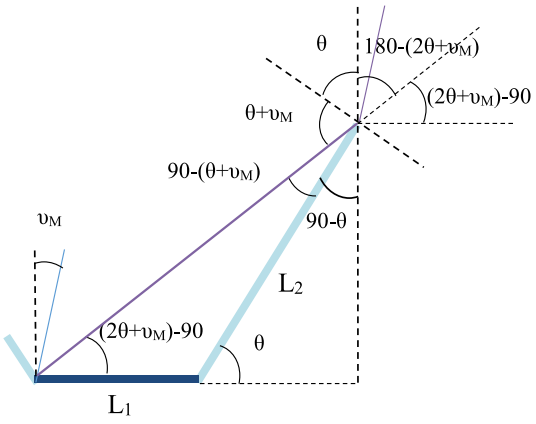

Fig. 4. Geometrical model of the concentrator (Hermenean et al., 2009).

Fig. 5. The location of experiment (Sofular Village, Tosya) and cities with similar climate in Turkey.

Here, $\tau_c = 0.90$, $\alpha_c = 0.95$, and $\delta_c = 0.90$ are PV module glass transparency, absorptivity of the solar cell, and the packing factor, respectively (Ceylan et al., 2016).

Electrical energy gain obtained from the PV module in the system can be calculated as follows. In this equation, $I_{(t)}$ is solar radiation falling into the PV module (W/m^2) and A_m is module surface area and equal to 0.416 m^2.

$$\dot{E}_l = \eta_m \cdot A_m \cdot I_{(t)} \tag{6}$$

The overall thermal energy gain is equal to the sum of the thermal energy gain and the thermal equivalent of the electrical

energy gain and can be calculated as follows.

$$\dot{Q}_{u,overall} = \dot{Q}_u + \frac{\dot{E}_l}{C_{power}} \tag{7}$$

In this equation, C_{Power} is used to convert electrical energy gain to thermal energy gain. C_{Power} is the coefficient of a thermal power plant that converts heat energy to electrical energy depending on the quality of the coal. C_{power} can be taken as 0.38 for a good quality coal that has low ash ratio. This value is between 0.20 and 0.40 (Huang et al., 2001; Ceylan et al., 2016). The overall thermal energy efficiency of the system can be calculated as follows. In this equation, W_{fan} is the energy consumed by the fans used in the system.

$$\eta_{overall} = \frac{\dot{Q}_{u,overall}}{A_m \cdot I_{(t)} - W_{fan}} \tag{8}$$

5. Exergy analysis

Exergy analysis relies on the second law of thermodynamics and accounts for the relation between the total input, output, and destroyed exergies. In general the exergy balance of a PV/T collector is given as follows (Dubey et al., 2009),

$$\sum \dot{E}x_{in} - \sum \dot{E}x_{out} = \sum \dot{E}x_{dest} \tag{9}$$

where the exergy output equals the sum of electrical energy gain and thermal exergies (Tiwari et al., 2018).

$$\sum \dot{E}x_{out} = \dot{E}x_{thermal} + \dot{E}_l \tag{10}$$

Exergy input of the system equals to the solar radiation exergy and the radiation energy is calculated by Petela as a function of ambient temperature and solar surface temperature as follows (Shukla et al., 2016; Öztürk and Kaya, 2013; Petela, 1964).

$$\sum Ex_{in} = I_{(t)} A_m \left[1 - \frac{4}{3} \cdot \frac{T_{amb}}{T_{sun}} + \frac{1}{3}\left(\frac{T_{amb}}{T_{sun}}\right)^4\right] \tag{11}$$

Here, T_{amb} is the ambient temperature and T_{sun} is the surface temperature of sun. Surface temperature of sun is taken as 5777 K (Park et al., 2014).

The thermal exergy of the system can be defined as the heat loss over the PV module to the surroundings (Tiwari et al., 2018; Sahota and Tiwari, 2017).

$$\dot{E}x_{thermal} = \dot{m} c_p \left\{(T_o - T_i) - (T_{amb} + 273)\ln\left(\frac{T_o + 273}{T_i + 273}\right)\right\} \tag{12}$$

Exergy efficiency is defined as the ratio of exergy output of the system to initial exergy input of the system. Exergy efficiency of a PV/T system is calculated as follows (Öztürk and Kaya, 2013; Joshi et al., 2009).

$$\eta_{exergy} = \frac{\dot{E}x_{out}}{\dot{E}x_{in}} \tag{13}$$

6. Enviroeconomic analysis

In this study, enviroeconomic analysis is carried out to see how much energy produced by solar energy in the system prevented CO_2 emissions. In calculations, CO_2 emissions are neglected during the fabrication and construction of the system. Enviroeconomic (environmental cost) analysis is made using carbon price (or CO_2 emission price) and the amount of CO_2 emission. Determination of a carbon price is an important tool in the mitigation of the national emission of greenhouse gases. Carbon price is an approach to calculate the cost of the emission of greenhouse gases that cause global warming. Paying the price of carbon (CO_2) released to the atmosphere will encourage people and countries to mitigate their carbon emissions. This will also reveal the significance of renewable energy technologies that do not release carbon to the atmosphere (Caliskan et al., 2012). Average equivalent CO_2 density to produce electricity from coal is given approximately as 960 g CO_2/kW h in an article published by Sovacool in 2008 (Sovacool, 2008). When the overall 40% loss in electric power transmission and distribution and 20% loss arising from inefficient electric instruments are considered, this value shall be 2.08 kg CO_2/kW h (Tripathi et al., 2016). Hence CO_2 mitigation in CPV/T air collector is given as follows

$$\phi_{CO_2} = \psi_{CO_2} \times \dot{Q}_{u,overall} \tag{14}$$

where ϕ_{CO_2} and ψ_{CO_2} signify the amount of CO_2 mitigation per hour (kg CO_2/h) and average amount of CO_2 emission during energy production out of coal (2.08 kg CO_2/kW h), respectively. Elzen et al. report that CO_2 price in 2011 was between 13 \$/t CO_2 and 16 \$/t CO_2 (Elzen et al., 2011). In calculations 1.45 ¢/kg CO_2 is used, the average of these values.

$$Z_{CO_2} = P_{CO_2} \times \phi_{CO_2} \tag{15}$$

where Z_{CO_2} and P_{CO_2} are, respectively, environmental cost (price of CO_2 reduction per hour, ¢/h) and carbon price per kg CO_2 which is taken as 1.45 ¢/kg CO_2.

7. Uncertainty analysis

The uncertainty analysis determines the accuracy limits of the given information. Considering the standard deviations of the measuring instrument used in the dryer, the uncertainties are calculated from Eqs. (16)–(20) and are given in Table 1.

$$X_m = \frac{1}{N}\sum X_i \tag{16}$$

$$V = \frac{1}{N-1}\sum \left(X_i{}^2 - X_m{}^2\right) \tag{17}$$

$$S = \sqrt{V} \tag{18}$$

$$a = \frac{1}{\sqrt{N}} \tag{19}$$

$$U = \sqrt{\sum_{i=1}^{R} a_i{}^2 \cdot S_i{}^2} \tag{20}$$

In equations, X_m is the arithmetic mean of observations, X_i is observations, N is number of observations, a is precision, S is standard deviation, V is variance and U is uncertainty (Gürel et al., 2015).

8. Evaluation and discussion

Solar radiation and concentrated solar radiation are measured during experiments and are plotted in Fig. 6a. Depending on the geometry of the concentrator, concentrating ratio has varied during the day and reached a maximum value of 1.8. Chamber and outdoor temperatures are measured in the experiments as well (Fig. 6b). As a result of the measurements, the outdoor temperature was around 10–12 °C while the heated space temperature was around 37 °C.

Depending on the temperature of the air entering and leaving the collector, the thermal energy gain in the system is calculated

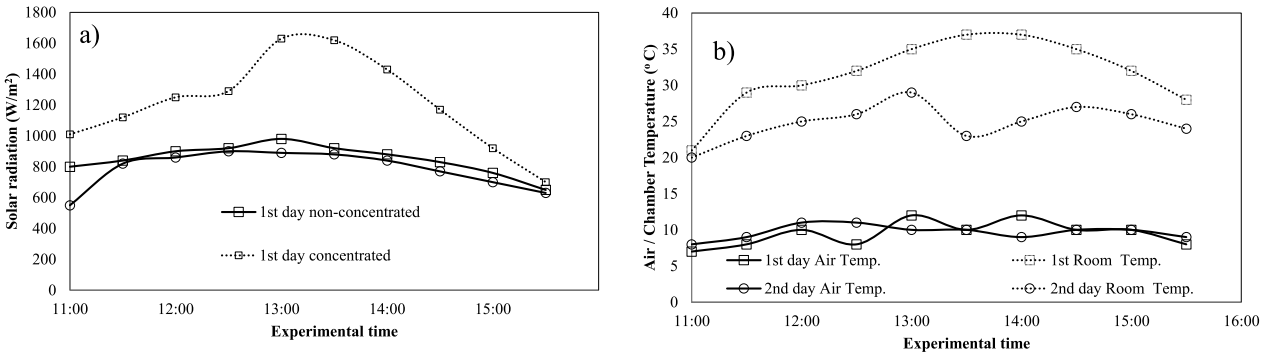

Fig. 6. Variation of solar radiation (a) and chamber temperature and ambient air temperature versus experimental time (b).

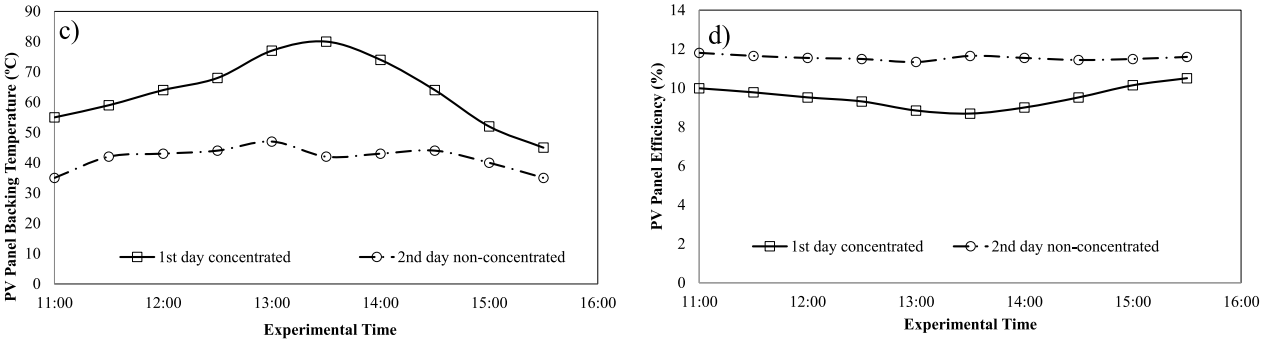

Fig. 7. Photovoltaic panel backing temperature and photovoltaic panel efficiency.

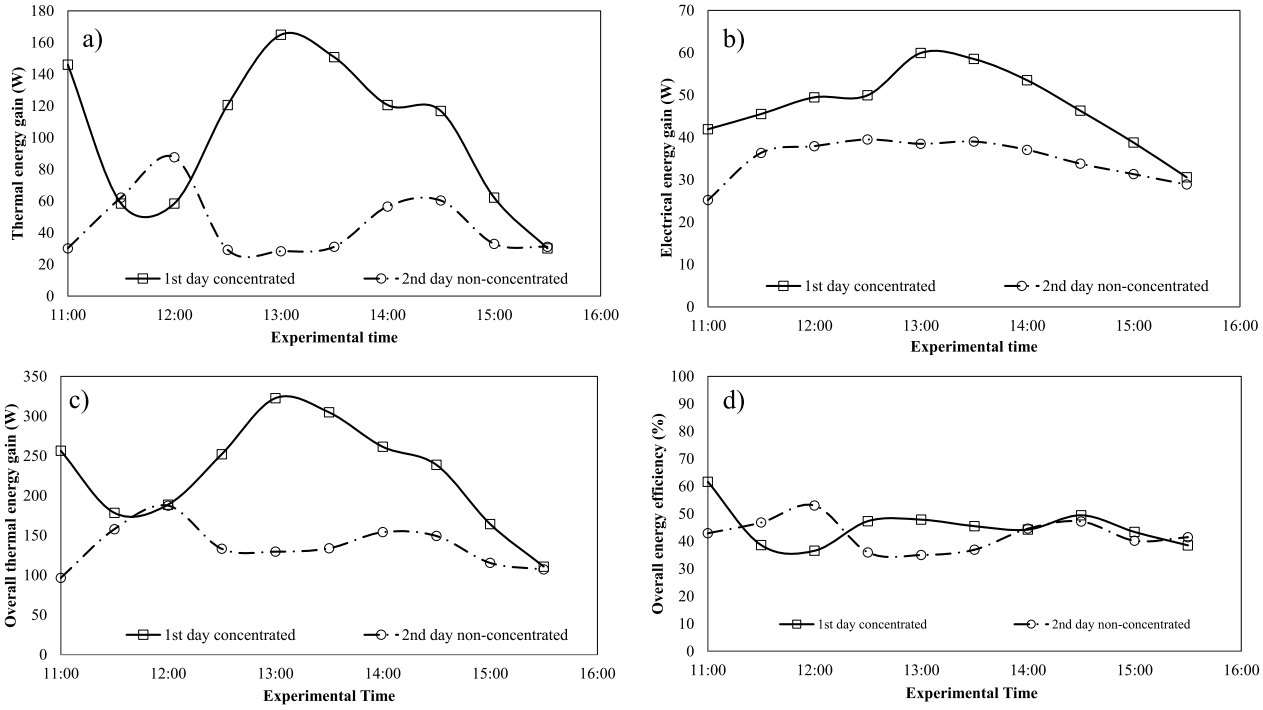

Fig. 8. Energy analysis graphs.

using Eq. (2) (Fig. 8a). Upon an inspection of the plot, one can realize that more thermal energy gain was obtained in the first day when the concentrator was in the system than in the second day when the concentrator was not used. Likewise, depending on concentrator's capacity to amplify solar radiation, electrical energy gain obtained from solar panel (It is generated 50 W at the laboratory conditions) has reached a level of 60 W for the day in which a concentrator was applied (Fig. 8b). Electrical energy gain is calculated through Eq. (6) and exhibited in Fig. 8b. Thermal and electrical energy gains in the system are added and overall thermal energy gain of the system is calculated via Eq. (7) and compared in Fig. 8c. The use of concentrator has increased the panel backing temperature. The variation of the panel backing temperature during the experiments is shown in Fig. 7a. The

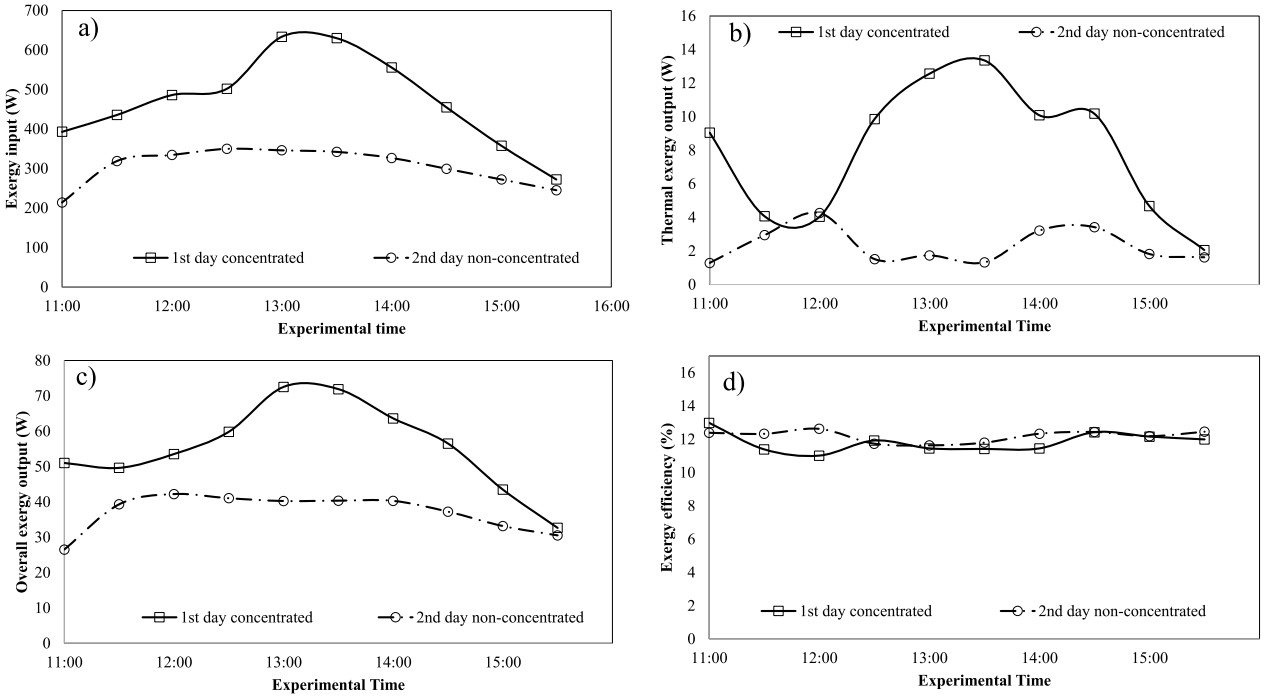

Fig. 9. Exergy analysis graphs.

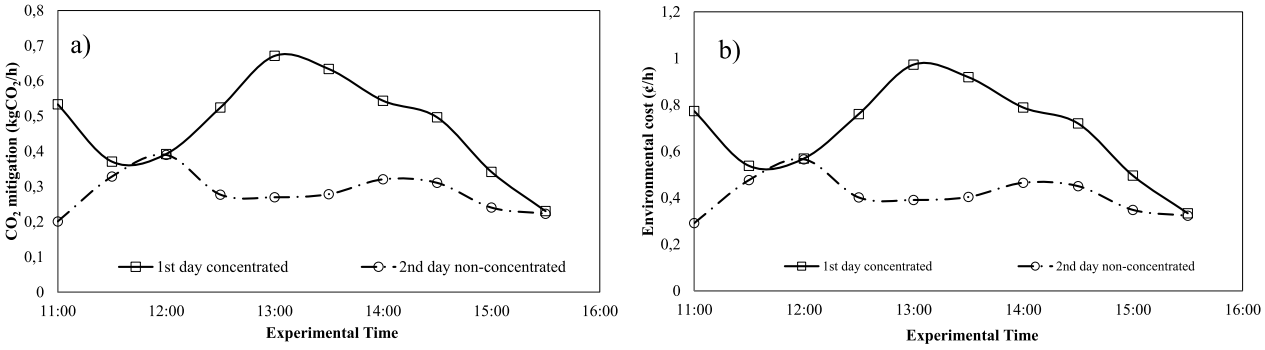

Fig. 10. Enviroeconomic analysis graphs.

electrical efficiency of the concentrating systems is lower than that of the non-concentrating systems due to the increase in the panel backing temperature. The variations in the electrical efficiencies with respect to the experimental time are shown in Fig. 7b. Although the efficiencies of the concentrating systems are low, their electrical gains are seen to be higher with respect to the concentrator-free systems in Fig. 8b. Efficiency concentrator is not an accurate indicator of the electrical gains of concentrating systems.

On the day when concentrator is used, it can be said that the overall thermal energy gain is about twice that of unused day. The overall thermal energy efficiency of the system is calculated using Eq. (8) in two ways by employing concentrating solar radiation and non-concentrating solar radiation values. The thermal energy efficiency of the system thus obtained is shown in Fig. 8d.

Exergy of solar radiation as well as the exergy input of the system have been calculated via Eq. (11) and exhibited in Fig. 9a. It can be said that the exergy input of the system has been doubled for the day where a concentrator has been employed. When the thermal exergy output was calculated via Eq. (12), results as exhibited in Fig. 9b have been obtained. Significant amount of thermal exergy output has been observed for the day in which a concentrator has been employed. Total exergy output of the system has been calculated as maximum 70 W. (see Fig. 9c). Exergy efficiency of the system has been calculated via Eq. (13) and the results have been displayed in Fig. 9d.

Enviroeconomic analysis is carried out by using the amount of released carbon and carbon price in this study. The amount of CO_2 mitigation of the system, which is a measure of the avoided amount of CO_2 that will be released due to coal use, is calculated using Eq. (14) and is shown in Fig. 10a. The environmental cost, a measure of the savings achieved due to the avoided production amount of CO_2, was calculated using Eq. (15) and is shown in Fig. 10b, as well. According to the results obtained, a CO_2 mitigation up to 0.6 kg per hour has been achieved and in return savings up to 1 ¢ per hour have been obtained.

9. Conclusions

The following conclusions and assessments can be withdrawn from the experimental studies and calculations that were carried out.

- Depending on the designed concentrator geometry, the concentration ratio increased 1.8 times during the hours in which the sun rays were received at near right angles.

- While the average outdoor temperature was measured as 10 °C during the tests, average supply air of concentrating system was measured as 32 °C and that of non-concentrating system was measured as 25 °C.
- The use of a concentrator in the system is very effective. When a concentrator was employed, thermal energy gain, thermal exergy output, electrical energy gain, and electrical exergy output rose.
- Thermal energy efficiencies of the system are at around 50%. The electrical efficiencies of concentrating systems are lower than those of non-concentrating systems. However, electrical gains are higher compared to systems is which a concentrator has not been employed. Efficiency for concentrating systems is not an accurate indicator of energy production.
- The exergy efficiency of the system has been calculated as 11%–12%.
- The use of concentrators has had a positive impact on the results of enviroeconomic analysis. The system savings have increased by about 50% as a result of CO_2 mitigation.

Experimental results show that the system is eco-friendly, and similar systems can be used in green building applications. The system can be used for preheating or heating in HVAC (Heating Ventilating and Air Conditioning) systems. Thermal storage systems can be integrated into the system so that the solar powered system can be used in cloudy weathers and nights.

Acknowledgment

This research was supported by Karabük University in Turkey under grant number KBÜBAP-17-DR-199.

References

Aldegheri, F., Baricordi, S., Bernardoni, P., Brocato, M., Calabrese, G., Guidi, V., Mondardini, L., Pozzetti, L., Tonezzer, M., Vincenzi, D., 2014. Building integrated low concentration solar system for a self-sustainable Mediterranean villa: The Astonyshine house. Energy Build. 77, 355–363.

Bhowmik, H., Amin, R., 2017. Efficiency improvement of flat plate solar collector using reflector. Energy Rep. 3, 119–123.

Caliskan, H., Dincer, I., Hepbasli, A., 2012. Exergoeconomic, enviroeconomic and sustainability analyses of a novel air cooler. Energy Build. 55, 747–756.

Ceylan, İ., Gürel, A.E., Ergün, A., Tabak, A., 2016. Performance analysis of a concentrated photovoltaic and thermal system. Sol. Energy 129, 217–223.

CLİMATE-DATA.ORG, 0000. [Online]. Available: https://tr.climate-data.org/location/17272/ [Accessed 16 11 2017].

Conventry, J.S., Franklin, E., Blakers, A., 2002. Thermal and electrical performance of a concentrating PV/Thermal collector: results from the ANU CHAPS collector. In: ANZSES Solar Energy Conference. Newcastle.

Dubey, S., Solanki, S., Tiwari, A., 2009. Energy and exergy analysis of PV/T air collectors connected in series. Energy Build. 41, 863–870.

Elzen, M.G.d., Hof, A.F., Beltran, A.M., Grassi, G., Roelfsema, M., Ruijven, B.v., Vliet, J.v., Vuuren, D.P.v., 2011. The Copenhagen accord: abatement costs and carbon prices resulting from the submissions. Environ. Sci. Policy 14, 28–39.

Gürel, A.E., Ceylan, İ., Yılmaz, S., 2015. Isı Pompalı ve Parabolik Oluklu Güneş Kolektörlü Akışkan Yataklı Kurutucuların Deneysel Analizi. Isı Bilimi ve Tekniği Derg. 35 (1), 107–115.

Halıcı, F., Gündüz, M., 2013. Örneklerle Isı Geçişi. Birsen Yayınevi, İstanbul.

Hermenean, I., Visa, I., Diaconescu, D., 2009. On the geometric modelling of a concentrating pv-miror system. Bull. Transilv. Univ. Brasov 2 (51), 73–80.

Huang, B., Lin, T., Hung, W., Sun, F., 2001. Performance evaluation of solar photovoltaic/thermal systems. Sol. Energy 70, 443–448.

Joshi, A.S., Dincer, I., Reddy, B.V., 2009. Thermodynamic assessment of photovoltaic systems. Sol. Energy 83, 1139–1149.

Joshi, A.S., Tiwari, A., 2007. Energy and exergy efficiencies of a hybrid photovoltaic–thermal (PV/T) air collector. Renew. Energy 32, 2223–2241.

Kong, C., Xu, Z., Yao, Q., 2013. Outdoor performance of a low-concentrated photovoltaic–thermal hybrid system with crystalline silicon solar cells. Appl. Energy 112, 618–625.

Marques, L., Torres, J.P.N., Branco, P.J.C., 2018. Triangular shape geometry in a Solarus AB concentrating photovoltaic-thermal collector. Int. J. Interact. Des. Manuf. (IJIDeM) 12 (4), 1455–1468.

Öztürk, H.H., Kaya, D., 2013. Güneş Enerjisinden Elektrik Üretimi: Fotovoltaik Teknoloji. Umuttepe Yayınları, Kocaeli.

Park, S., Pandey, A., Tyagi, V., Tyagi, S., 2014. Energy and exergy analysis of typical renewable energy systems. Renew. Sustain. Energy Rev. 30, 105–123.

Petela, R.R., 1964. Exergy of heat radiation. ASME J. Heat Transfer 86 (2), 187–192.

Sahota, L., Tiwari, G., 2017. Review on series connected photovoltaic thermal (PVT) systems: analytical and experimental studies. Sol. Energy 150, 96–127.

Sharma, S., Tahira, A., Reddy, K., Mallick, T.K., 2016. Performance enhancement of a building-integrated concentrating photovoltaic system using phase change material. Sol. Energy Mater. Sol. Cells 149, 29–39.

Shukla, A.K., Sudhakar, K., Baredar, P., 2016. Exergetic assessment of BIPV module using parametric and photonic energy methods: a review. Energy Build. 119, 62–63.

Sovacool, B., 2008. Valuing the greenhouse gas emissions from nuclear power: a critical survey. Energy Policy 36, 2940–2953.

Tiwari, G., Meraj, M., Khan, M., 2018. Exergy analysis of n-photovoltaic thermal-compound parabolic concentrator (N-PVT-CPC) collector for constant collection temperature for vapor absorption refrigeration (VAR) system. Sol. Energy 173, 1032–1042.

Tripathi, R., Tiwari, G., Dwivedi, V., 2016. Overall energy, exergy and carbon credit analysis of N partially covered photovoltaic thermal (PVT) concentrating collector connected in series. Sol. Energy 136, 260–267.

Xu, G., Zhang, X., Deng, S., 2011. Experimental study on the operating characteristics of a novel low-concentrating solar photovoltaic/thermal integrated heat pump water heating system. Appl. Therm. Eng. 31 (17-18), 3689–3695.